Model analysis of a double stage Hall effect thruster with double-peaked magnetic field and intermediate electrode

IEPC-2007-121

Presented at the 30th International Electric Propulsion Conference, Florence, Italy
September 17-20, 2007

J. Pérez-Luna*, G.J.M. Hagelaar†, L. Garrigues‡, and J.P. Boeuf§
LAboratoire PLAsma et Conversion d'Energie, LAPLACE
CNRS – Université Paul Sabatier, 118 Route de Narbonne, 31062 Toulouse cedex 9, France

A hybrid fluid-particle model has been used to study the properties of a double stage Hall effect thruster where the channel is divided into two regions of large magnetic field separated by a low field region containing an intermediate, electron-emitting electrode. These two features are aimed at separating effectively the ionization region from the acceleration region, in order to extend the thruster operating range. The simulations show good general thruster performances throughout a wide operating range. However, they question a complete separation of the ionization and acceleration regions and the necessity of an electron-emissive intermediate electrode. The calculation method for the electric potential in the hybrid model has been improved with respect to our previous work and is capable of a complete two-dimensional description of the magnetic configurations of double stage Hall effect thrusters.

Nomenclature

$\boldsymbol{\Gamma_e}$	=	electron flux
$\boldsymbol{\Gamma_i}$	=	ion flux
N	=	atom density
n	=	plasma density
S	=	source term
ε	=	electron mean energy
$\boldsymbol{E}$	=	electric field
$\boldsymbol{B}$	=	magnetic field
$\boldsymbol{\omega}$	=	cyclotron frequency
V	=	electric potential
V_i	=	potential drop between anode and IE
V_a	=	potential drop between IE and cathode
μ	=	electron mobility
$\mu_\perp$	=	cross-field electron mobility
k_i	=	ionization coefficient
e	=	elementary charge
m_e	=	electron mass
κ, W	=	energy loss coefficients

* PhD. student, perezluna@laplace.univ-tlse.fr
† Research scientist, hagelaar@laplace.univ-tlse.fr
‡ Research scientist, garrigues@laplace.univ-tlse.fr
§ Senior scientist, jpb@laplace.univ-tlse.fr

ν_m = total momentum-transfer frequency
ν_c = classical momentum-transfer frequency
ν_b = bohm momentum-transfer frequency
k_{in}, k_{out} = mobility fitting parameters
α_ε, U = energy fitting parameters
$\dot{m}$ = Xenon mass flow rate
T = thrust
Isp = specific impulse
η_d = discharge efficiency

I. Introduction

In Hall Effect Thrusters (HET) an ion beam can be extracted at high speed without extracting grids (i.e. without space charge limitation), leading to high specific impulse (Isp). However, Isp and thrust cannot be controlled separately in standard, single stage HET. Space missions necessitate often a versatile propulsive system capable of being efficient in a high specific impulse and in a high thrust mode[1]. This is the case for telecom satellites which have conflicting needs for station-keeping and orbit transfer sequences. It is also the case for many scientific missions which require high impulse during interplanetary cruise and high thrust for Earth escape and final orbit acquisition around the target planet[2]. A thruster capable of being efficient in a wide operating range would combine the advantages of both HET and Gridded Ion Engines (GIE)[3].

A possible answer to these requirements is the Double Stage Hall Effect Thruster (DSHET) concept. This variant could provide a wide range of specific impulse and thrust and operating powers in a wide range at constant specific impulse. The idea in DSHETs is to separate the ionization region from the acceleration region. This way, for a given power, the thruster can operate in a high Isp or a high thrust regime. A great effort was made by TsNIIMASH during the 1960s and 1970s concerning two-stage high power thrusters, but electric thrusters research in former Soviet Union gradually shifted to single-stage, low power thrusters. Since the 1990s, TsNIIMASH and NASA have recovered two-stage thrusters investigation[4]. In Europe, SNECMA has also looked into a DSHET concept based on the semi-Galathea magnetic field configuration[5]. We have studied this concept with the help of hybrid models, and a detailed modelling study of this thrusters will be published elsewhere. A review of two-stage Hall thrusters is provided by *Hofer et al*.[6]. There are only a few publications concerning double-stage thrusters simulations. One of them is the paper of *Ahedo et al*[7] in which an exhaustive numerical study of the influence of a third electrode in the discharge channel of a HET is presented.

In this paper we study the DSHET concept proposed by Alcatel Alenia Space Italia (AASI) (Florence plant) and Alta S.p.A.[8]. This DSHET has a geometry similar to standard HETs but two features have been added to allow double stage operations by decoupling the ionization and acceleration regions: 1) the magnetic field presents two maxima in the channel (with a zero magnetic field and a separatrix), and 2) an intermediate, emissive electrode is placed in the region between the two magnetic field maxima. The purpose of the work is to analyze, with the help of a 2D hybrid model, the properties of this thruster and its ability to efficiently operate as a double stage thruster. Section II presents an overview of the hybrid model and its recent improvements. The operations of the thruster in

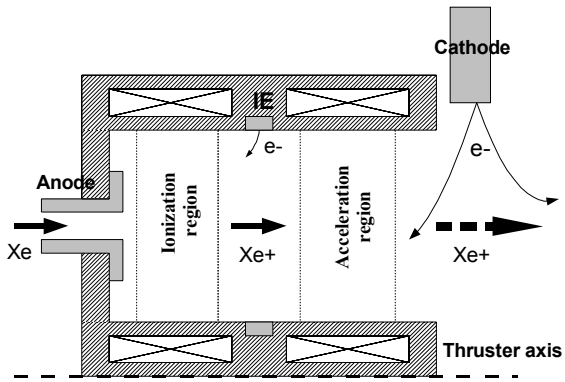

Figure 1: Schematic view of the DSHET with the Intermediate Electrode (IE) and the four coils configuration.

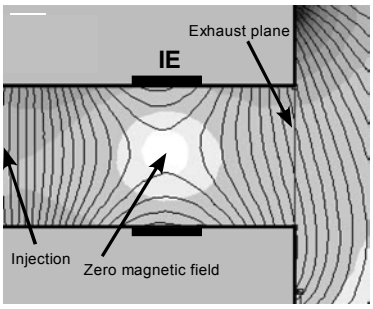

Figure 2: Double stage 2D magnetic field configuration and lines – the zero magnetic field is visible in the middle of the channel.

single and double stage regimes are described and discussed in Section III. Section IV summarizes the main conclusions.

II. DSHET concept

A. Geometry and Intermediate Electrode

The thruster geometry is very similar to that of a typical HET (Fig.1). The DSHET is a cylindrical thruster with a single discharge chamber bordered by ceramic walls. At the inner bound of the chamber are the anode and the gas distributor. Outside the channel is the external cathode. One of the differences between this DSHET and a standard thruster is the intermediate electrode (IE) in the middle of the channel. This electrode is formed by four equidistant in azimuthal direction and equipotential electrodes positioned around the external chamber wall. The seond difference with standard HET is the presence of four cylindrical coils surrounding the discharge channel. These four coils are designed to control independently the magnetic field in the anode-IE region and in the IE-cathode region.

These specific features are included to enable the separation of the ionization and acceleration regions, which makes this thruster a DSHET. The efficiency of this separation will be discussed later in the paper. The ionization region stands between the anode and the intermediate electrode and the acceleration region is located between the IE and the cathode. Electrons are emitted by the external cathode and are first trapped in the acceleration region magnetic field peak. The potential drop in the acceleration region is determined by the fixed potentials of the IE and the cathode. The Xenon injected at the anode is ionized between the anode and the IE. In the original concept, the IE is emissive and can provide, if needed, an electron current for the Xenon ionization. The potential drop in this area is also determined by the fixed potential of the anode and the IE. Xenon ions are finally accelerated in the acceleration region.

B. Magnetic circuit and configurations

The magnetic circuit of the thruster is made out of steel. The four-coil system can provide a simple peaked magnetic field if only the front coils are on or if the four of them are similarly polarized. But it can also provide a double peaked magnetic field if the rear and front coils are oppositely polarized (Fig.2). Moreover these four coils are useful to adjust precisely the magnetic peak values and the inclination of the magnetic lenses in the acceleration and ionization regions. The results presented in this article correspond to nominal configurations.

III. Overview of the hybrid model and improvements

A. Overview

The model is based on the hybrid fluid-particle model of a HET described in previous publications[9,10] and has been developed in the frame of the CNRS/CNES/SCNEMA Research Group on Space Propulsion. We recall below the basic ideas and assumptions of the model and present some recent improvements related to the electric field calculation. The model assumes azimuthal symmetry and the computational domain includes both the discharge channel and the near exterior of the thruster. The density of neutral xenon atoms in the thruster is obtained from a particle simulation. The neutrals are introduced in the simulation at a certain injection region at the anode and are followed until they reach the right boundary of the geometry. Additional neutrals are introduced at the channel walls to account for wall-recombination of ions. Only collisions with walls are considered, in which the neutrals are isotropically scattered. Like the neutrals, the ions are described by a particle simulation. They are followed until they

reach any of the boundaries of the simulation domain; ions striking the walls are thus assumed to recombine at the surface. In this study, the model assumes all ions to be singly charged. The model describes the electrons by a set of fluid equations.

The electric potential distribution is obtained from the electron momentum transfer equation and assuming quasineutrality of the plasma. The three electron fluid transport equations used in the model are shown below. The continuity equation (current conservation) is:

$$\nabla \cdot \mathbf{\Gamma}_\mathbf{e} = Nnk_i - \frac{\partial n}{\partial t} = \nabla \cdot \mathbf{\Gamma}_i \tag{1}$$

the momentum equation is written in the drift-diffusion form:

$$\mathbf{\Gamma}_e = -\mu \mathbf{E} n - \frac{2}{3e}\mu \nabla(n\varepsilon) \tag{2}$$

and the energy equation is written as:

$$\frac{\partial(n\varepsilon)}{\partial t} + \frac{5}{3}\nabla \cdot (\mathbf{\Gamma}_\mathbf{e}\varepsilon) - \frac{10}{9e}\nabla \cdot (\mu n \varepsilon \nabla \varepsilon) = -e\mathbf{E} \cdot \mathbf{\Gamma}_\mathbf{e} - Nn\kappa - nW \tag{3}$$

In these equations n is the plasma density, $\mathbf{\Gamma_e}$ the electron flux, ε the electron mean energy, N the gas density, $\mathbf{\Gamma_i}$ the ion flux, $\mathbf{E}$ the electric field, μ the electron mobility, k_i the ionization coefficient and e the elementary charge. The last two terms in the energy equation represent energy loss by collisions with gas particles and with the walls, respectively, where κ and W are effective energy loss coefficients. Equations (2) and (3) assume that the electron distribution is Maxwellian and predominantly isotropic; this assumption is used to obtain the collision coefficients k_i and κ from cross section data. Due to the magnetic field the mobility is a tensor: its value is much larger for electron transport along magnetic field lines than for transport across them.

B. Improvement of the electric potential calculation

In previous papers[9,10] we assumed that electrons were in Boltzmann equilibrium along the magnetic field and the potential distribution across the magnetic field lines was deduced from a resulting 1D momentum transfer equation for the electrons. In this paper we no longer assume Boltzmann equilibrium along the magnetic field lines and the potential distribution is obtained from the full axial and radial components of equation (2):

$$\Gamma_x = \frac{\nu^2 + \omega_x^2}{\nu^2 + \omega^2}\left[\mu n \frac{\partial V}{\partial x} - \frac{2}{3e}\mu \frac{\partial(n\varepsilon)}{\partial x}\right] + \frac{\omega_x \omega_y}{\nu^2 + \omega^2}\left[\mu n \frac{\partial V}{\partial y} - \frac{2}{3e}\mu \frac{\partial(n\varepsilon)}{\partial y}\right] \tag{4}$$

$$\Gamma_y = \frac{\nu^2 + \omega_y^2}{\nu^2 + \omega^2}\left[\mu n \frac{\partial V}{\partial y} - \frac{2}{3e}\mu \frac{\partial(n\varepsilon)}{\partial y}\right] + \frac{\omega_x \omega_y}{\nu^2 + \omega^2}\left[\mu n \frac{\partial V}{\partial x} - \frac{2}{3e}\mu \frac{\partial(n\varepsilon)}{\partial x}\right] \tag{5}$$

where $\boldsymbol{\omega} = \frac{e\mathbf{B}}{m}$, ν is the electron collision frequency and $\mu = \frac{e}{m_e \nu}$ the mobility without magnetic field.

These expressions of the components of the electron flux are injected in the continuity equation (1) above. Knowing the plasma density and ion flux from the particle description of the ion transport, the resulting equation is an elliptic equation for the potential. This elliptic equation is strongly anisotropic, and is solved using a new efficient numerical algorithm[11].

C. Cross field electron mobility and electron-wall interactions

Cross field electron mobility is the main parameter controlling the electric potential distribution in the SPT and has therefore a major influence on the simulation results. Unfortunately this coefficient is not well known and it has been shown that electron-atom collisions are not sufficient to explain the observed electron conductivity in a HET[12]. The cross field electron mobility $\mu_\perp$ is related to the momentum-transfer frequency of electron-particle collisions ν_m as follows:

$$\mu_\perp = \frac{e\nu_m / m_e}{\nu_m^2 + (eB/m_e)^2} \approx \frac{m_e \nu_m}{eB^2} \tag{6}$$

where m_e is the electron mass. The model takes the momentum-transfer rate frequency to be constant at 2.5×10^{-13} m^3s^{-1}. This frequency is too small to be realistic for the electron transport in SPTs, especially near and beyond the exhaust where the gas density is very low. In previous papers the anomalous electron conductivity inside the channel was supposed to be due to electron-wall collisions[13,14]. Recent measurements[15] and calculations[16] have cast some doubts on this assumption and we assume in the present paper that the anomalous conductivity is only due to field fluctuation (Bohm conductivity) both inside and outside the thruster channel. The model therefore adds to the classical momentum-transfer rate frequency an anomalous Bohm frequency:

$$\nu_m = \nu_c + \nu_b = \nu_c + \frac{k\omega}{16} \tag{7}$$

where k is a constant fitting parameter. Anomalous Bohm momentum-transfer frequency is applied inside and outside the channel with different fitting parameters: k_{in} and k_{out} with $k_{in}<k_{out}$ (this is necessary to obtain a good fit with experiments).

Although it seems from Refs[15,16] that electron-wall collisions do not play an important role in the electron momentum exchange, they may significantly contribute to the overall electron-energy exchange. The fluid model shows that energy losses due to electron-atom collisions are not sufficient to reproduce experimental results and that energy losses that can be estimated with simple wall sheath model[16] provide reasonable results. To represent these losses, we use in the present paper the same empirical energy loss coefficient as in Refs.[9,10,13]. The energy loss per second per electron is taken as

$$W = \alpha_\varepsilon 10^7 \varepsilon \exp(-\frac{U}{\varepsilon}) \tag{11}$$

where α_ε and U are constant fitting parameters, set to α_ε=1.2 and U=20eV in both cases of this study.

IV. Simulation results for single and double stage operations

A. Single stage (SS) operation

In single stage configurations, the DSHET is supposed to operate as a conventional HET. The IE is off and the magnetic field is single peaked. The nominal SS configuration corresponds to a 350V discharge voltage and a 4.7 $mg.s^{-1}$ mass flow rate. Our previous work[10] evidenced that for a very similar thruster, in a similar configuration (including magnetic field distribution), k_{in}=0.1, k_{out}=0.2 and α_ε=0.7 was the optimum triplet when optimizing simulated results with thruster performance, dynamic behaviour and potential distribution measurements. We therefore chose these coefficients as a start point. Experimental results provided by AASI (Florence) and Alta S.p.A.(Refs. [17,18], and personal communications with M. Capacci from AASI) were compared with simulation results. This comparison showed that the electron current and energy losses were too low. We therefore increased the mobility and energy losses, keeping the same inner/outer mobility ratio and obtained good agreement with experimental results for k_{in}=0.15, k_{out}=0.3 and α_ε=1.2.

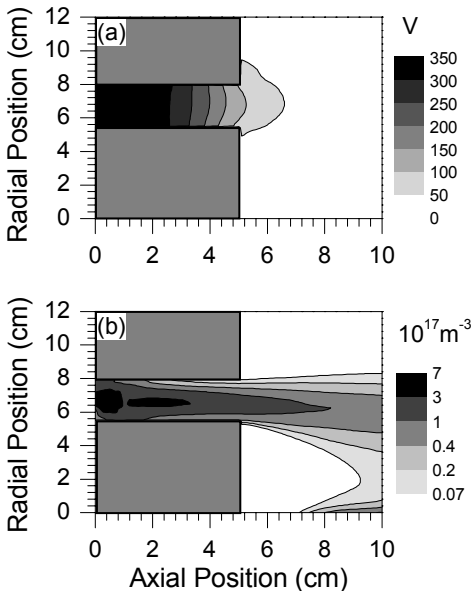

Figure 3 : a) potential (V) and b) plasma density ($\times10^{17}$ m^{-3}, log scale) for a nominal single stage mode simulation: mass flow rate 4.7 $mg.s^{-1}$ and Vd=350V.

The calculated 2D potential and plasma density distributions are presented in Fig.3. The potential decreases mainly inside the channel and the acceleration region is located between x=2.5cm and x=5cm. The maximum energy (about 14eV) is reached in this acceleration region, just before the ionization region. The gas is ionized in the first half of the channel (near the anode). At the exhaust, the jet is not straight and is deflected towards the axis, because of the magnetic lens inclination. In this single stage configuration, the model predicted a 70mN thrust and 1526s Isp (specific impulse) with an efficiency of about 40%.

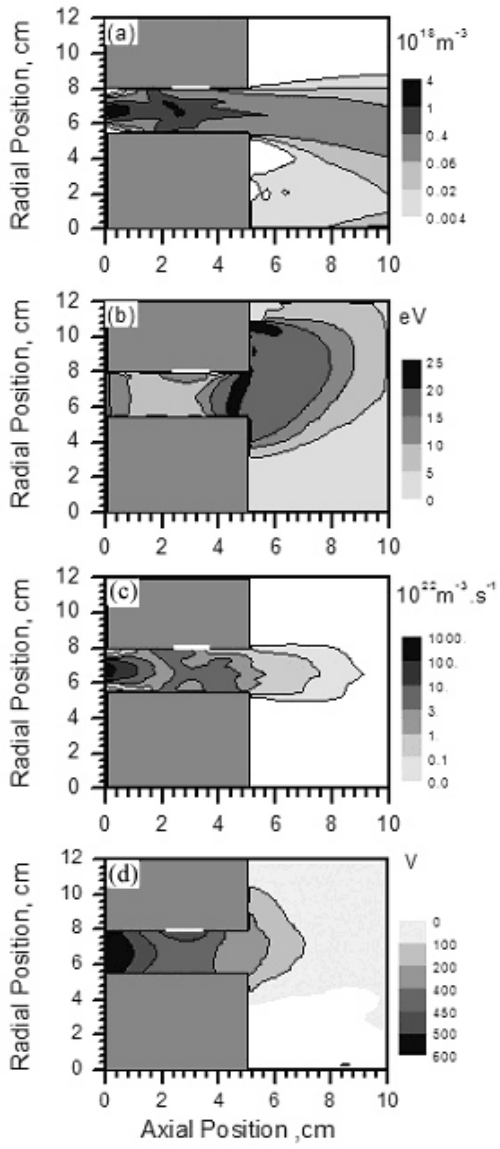

Figure 4 : 2D plasma characteristics in the case: V_i=100V, V_a=500V and a mass flow rate of 10 mg.s^{-1}; a) plasma density (×10^{18} m^{-3}. log scale); b) electron energy (eV); c) ionization source term (×10^{22} m^{-3}.s^{-1}, log scale); e) potential (V) - the white box represents the intermediate electrode.

B. Double Stage (DS) operation

In double stage configurations, the intermediate electrode potential is set to a chosen value. Before presenting the results, we must here point out that the IE potential and current can not be both fixed in the simulations. The electrode potential is set to the chosen value and the simulation returns the calculated current.

As it was done for single stage configurations, different coefficients were compared with experimental data in order to choose the most accurate k_{in} and k_{out} parameters. Table 1 shows some of the studied cases which led to choose k_{in}=0.1, k_{out}=0.2 and α_ε=1.2. In the DSHET configuration, the magnetic field is double peaked. The peaks are determined by the coil currents. The simulation results presented here were obtained with a same magnetic field configuration corresponding to Fig. 2. We present in this section the plasma properties as predicted by the model in a typical case, for the following conditions: $\dot{m} = 10$ mg.s^{-1}, V_i=100V and V_a=500V, where V_i is the potential difference between the anode and the IE, and V_a between the IE and the cathode. Fig.4a and 4c show the plasma density and ionization source term respectively. The ionization region appears on the plot of the source term (ionization rate): $S=N_a n k_i(\varepsilon)$, where N_a is the atom density, n the plasma density and k_i the ionization coefficient which depends of the electron energy ε. Because the magnetic field is large and maximum at the anode, the axial electric field is also large in this region (reduced electron conductivity). Therefore the electron energy (Fig.4b) and ionization source term are large at the anode, which leads to a maximum in plasma density. The large ionization and plasma density next to the anode and gas injection can possibly lead (assuming that the model predictions are correct) to anode heating, discharge instabilities and wall erosion.

The potential distribution (Fig.4d) is as expected: 1) a potential drop between the anode and the IE absciss, associated with the electric field induced by the large magnetic field in that region, 2) a low electric field region in the zero magnetic field region around the IE, and 3) a second potential drop corresponding to the usual acceleration zone. We also notice that the potential around the IE is significantly below the IE potential (i.e. plasma potential is around 450 V while IE potential is set to 500 V). If we compare the potential and the source term profiles, we see that the acceleration and ionization regions are only partially separated. Atom wall recombination is one reason for this.

The electron mean energy distribution of Fig.4b is consistent with the potential distribution. There is a large maximum of the electron energy (25 eV) in the acceleration region, associated with the large potential drop distributed between the cathode and the IE region. The electron energy then decreases in the IE region because of the low electric field there, and increases again radially and axially.

Table 1: Comparison between experimental[17,18] (exp) and simulation (mod) data in different double stage configurations. V_a is the potential difference between the IE and the cathode and V_i between the anode and the IE. ε is the variation between experiment and simulation. k_{in}=0.1 and k_{out}=0.2. η_d is the discharge efficiency.

Flow rate	V_a	V_i	I_d		ε	T		ε	ISP		ε	η_d		ε
mg.s^{-1}	V	V	A		%	mN		%	s		%			%
			exp	mod		exp	mod		exp	mod		exp	mod	
10	350	50	9	8.8	2%	195	192	2%	1910	1880	1%	0.51	0.5	1%
10	250	50	9	7.9	12%	170	152	11%	1670	1490	11%	0.51	0.47	9%
7	350	50	6.1	5.8	5%	127	128	1%	1750	1770	1%	0.45	0.48	7%
4	350	50	3.3	2.87	13%	73	61	16%	1690	1570	7%	0.46	0.37	20%

Table 2: Calculated current collected by the intermediate electrode for different operating points of the DSHET.

CASE	$\dot{m}$ (mg.s^{-1})	V_i(V)	V_a(V)	I_{IE}(A)
1	10	30	500	2.92
2	10	100	500	2.26
3	10	30	700	3.23
4	18	30	375	4.73
5	18	50	375	3.99
6	18	100	375	2.95

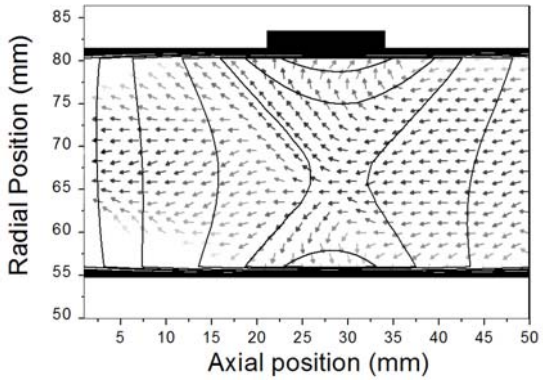

Figure 5: Electrons flow in channel for a double stage configuration (10 mg.s^{-1}, V_i=100V and Va=500V). Black lines show some magnetic field lines. The intensity of the flux is indicated by the grey level of the arrows (darker arrow corresponds to a larger flux. maximum value 10^{22} m^{-2}.s^{-1})

C. Role of the intermediate electrode and separation of ionization and acceleration in the DSHET

The intermediate electrode plays a major role in the thruster behaviour. It fixes the plasma potential in its vicinity and controls the current. Table 2 shows the current received by the external wall in all of the double stage configuration cases. The model predictions indicate that the IE never acts as an emissive electrode in the simulated cases, and acts as an anode rather than a cathode. The IE collects an electron current between 2A and 5A in the conditions of the simulations. This means that the electrode current supplied by the cathode is sufficient to maintain quasi-neutrality in the channel. We were able to find conditions were the IE would act as an emissive electrode, i.e. where the model predicted a current from the electrode, but these conditions corresponded to a very large applied potential between the IE and the anode (V_i>300V), which was not consistent with the expected regime of operation of the thruster.

Figure 5 can help understand the plasma properties and current distribution in the region around the IE. This figure shows the electron flux in the discharge chamber and the magnetic field lines. The current direction is indicated by the arrows and its intensity by a grey colour scale. We see that some of the electrons coming from the acceleration region on the right of the plot are collected by the intermediate electrode. We also note an increase of the electron current between the IE and the anode, due to ionization in that region. The flux is maximum in the zero magnetic field area (where the electron mobility is maximum) and near the anode. Near the IE, the electrons clearly follow the magnetic field lines; this explains why we find a large collected current by the IE in Table 2.

V. Conclusion

The AASI DSHET operations have been simulated with the hybrid model developed in the frame of the CNRS/CNES/SCNEMA Research Group on Space Propulsion. The magnetic field calculations show that the four coil configuration of the thruster provides some flexibility to control the magnetic field distribution, and allow single stage or double stage operations.

In single stage operating modes, the model can reproduce the main measured characteristics of the thrusters provided that anomalous transport coefficients are adjusted. In double stage operations, the performances predicted by the model are similar to the measured ones in high power configurations but are smaller in low power configurations.

A closer look at the 2D discharge features showed that the thruster's theoretical concept, in the investigated geometry, is partially verified and margins for improvements still exist. For instance the ionization region and the acceleration region are indeed partially separated, i.e. can be controlled separately, but ion recombination at the walls prevents a complete separation. Also the model tends to predict high plasma density and electron temperature near the anode in double stage operation. A last major issue is the role of the intermediate electrode. The model predicts that the intermediate electrode is actually not emissive in most conditions and it is therefore not clear whether or not this thruster really operates in a regime where an emissive electrode is needed.

Acknowledgments

This DSHET concept has been developed by Alcatel Alenia Space Italia (AASI) and ALTA S.p.a (as main sub-contractor) under ESA/ESTEC contract (n. 16724/02/NL/CP). The authors would like to thank M. Capacci (Florence plant) for helpful discussions and M. Gengembre from ESA for his support. The model development has been performed in the frame of the Groupement De Recherche CNRS/CNES/SNECMA/Universités n°2759 "Propulsion Spatiale à Plasma". J. Perez Luna benefits from a CNES/SNECMA PhD fellowship.

[1] Oleson S.R., "Electric Propulsion For Low Earth Orbit Communication Satellites", *25th International Electric Propulsion Conference*, Cleveland, OH, IEPC-97-148, 1997.

[2] Koppel C.R., Marchandise F., Prioul M., Estublier D., and Darnon F., "The Smart-1 Electric Propulsion Subsystem Around the Moon: In Flight Experience", *41st AIAA Joint Propulsion Conference*, Tucson, AZ, paper AIAA-05-3671, 2005.

[3] Zhurin V.V., Kaufman H.R., and Robinson R.S., "Physics of closed drift thrusters", *Plasma Sources Sci. Technol.*, Vol. 8, R1-R20, 1999.

[4] Tverdokhlebov S.O, "Study of Double-Stage Anode Layer Thruster Using Inert Gases", *23rd International Electric Propulsion Conference*, Seattle, WA, paper IEPC-93-232, 1993.

[5] M. Prioul, P. Dumazert, A.I. Bugrova, A.I. Morozov, V.K. Harchevnikov, A.V. Desyatskov, M.V. Kozintceva, V.V. Saveleiev, L. Jolivet, E. Gengembre, E. Chesta, J.P. Boeuf, C. Boniface, R. Rigollet, M. Saverdi, F. Castro, H. Simpson, *in Proceedings of the 4th International Spacecraft Propulsion Conference,* Chia Laguna (Cagliari), Italy, (Editor: A.Wilson. Published on CDROM., p.33.1, 2004), ESA SP-555.

[6] Hofer R.R., Peterson P.Y, Gallimore A.D., and R.S. Jankovsky, "A High Specific Impulse Two-stage Hall Thruster with Plasma Lens Focusing", *27th International Electric Propulsion Conference*, Pasadena, CA, paper IEPC–01–36, 2001.

[7] Ahedo E. and Parra F.I., "A model of the two-stage Hall thruster discharge", *J. Appl. Phys*., Vol. 98, No. 023303, 2005.

[8] M. Cappaci, G. Matticari, G.E. Noci, P. Siciliano, M. Berti, L. Biagoni, U. Cesari, E. Gengembre, E. Chesta, "Development of a Double Stage Hall Thruster for Advanced Telecom, Remote Sensing and Scientific. Space Missions", *40th AIAA Joint Propulsion Conference*, Fort Lauderdale, paper AIAA-2004-3771, 2004.

[9] Hagelaar G.J..M., Bareilles J., Garrigues L., and Boeuf J.P., "Two-dimensional Model of a Stationary Plasma Thruster", *J. Appl. Phys*., Vol. 91, No. 9, pp. 5592-5598, 2002.

[10] Hagelaar G. J. M., Bareilles J., Garrigues L., and Boeuf J. P., "Role of anomalous electron transport in a stationary plasma thruster simulation", *J. Appl. Phys*., Vol. 93, No. 1, pp. 67-75, 2003.

[11] Hagelaar G.J.M., "Modelling electron transport in magnetized low-temperature discharge plasmas", *Plasma Sources Sci. Technol.*, Vol. 16, S57-S66, 2007.

[12] Morozov, A.I., Esinchuk, Y.V., Tilinin, G.N., Trofimov, A.V., Sharov, Y.A., and Shchepkin, G.Y., "Plasma Accelerator with Closed Electron Drift and Extended Acceleration Zone," *Soviet Physics Technical Physics*, Vol. 17, No. 1, pp. 38–45, 1972.

[13] Bareilles J., Hagelaar G. J. M., Garrigues L., Boniface C., Boeuf J. P., and Gascon N., "Critical assessment of a two-dimensional hybrid Hall thruster model: Comparisons with experiments", *Phys. Plasmas,* Vol. 11, No. 6, pp. 3035-3046, 2004.

[14] Barral S., Makowski K., Peradynski Z., Gascon N., and Dudeck M., "Wall material effects in stationary plasma thrusters. II. Near-wall and in-wall conductivity", Phys. Plasmas, Vol. 10, No. 10, pp. 4137-4152, 2003.

[15] C. Boniface, L. Garrigues, G. J. M. Hagelaar, J. P. Boeuf, D. Gawron, and S. Mazouffre, "Anomalous cross field electron transport in a Hall effect thruster", *Appl. Phys. Lett*., Vol. 89, No. 161503, 2006.
[16] Garrigues L., Hagelaar G.J.M., Boniface C., and Boeuf J.P., "Anomalous conductivity and secondary electron emission in Hall effect thrusters", *J. Appl. Phys*., Vol. 100, No.123301, 2006.
[17] P. Rossetti, U. Cesari, M. Saverdi, M. Capacci, P. Siciliano, G. Noci and E. Gengembre, "Experimental Characterization of a Double-Stage Hall Effect Thruster", *41st AIAA Joint Propulsion Conference*, Tucson, paper AIAA-2005-3879, 2005.
[18] P. Rossetti, M. Capacci, and G. Noci, "Preliminary Experimental Results on a Double Stage Hall-Effect Thruster", *42nd AIAA Joint Propulsion Conference*, Sacramento, paper AIAA-2006-4998, 2006.